Chapter

Exchange Bias Effect in Ni-Mn Heusler Alloys

Esakki Muthu Sankaran and Arumugam Sonachalam

Abstract

In this chapter the exchange bias (EB) properties of bulk Mn-rich $Ni_{50-x}Mn_{37+x}Sn_{13}$ ($0 \leq x \leq 4$) Heusler alloys has been discussed by changing the Ni-Mn concentration. In these alloys the exchange bias field increases with the excess Mn concentration, but exchange bias blocking temperature (T_{EB}) decreases from 149 to 9 K. The hysteresis loop for $Ni_{46}Mn_{41}Sn_{13}$ alloy shows a maximum shift of 377 Oe. The exchange bias property is strongly influenced by varying Ni-Mn concentration in Ni-Mn-Sn alloys then the variation of Mn/Sn. We have observed in these alloys that the T_{EB} would show a decreasing value either by changing the Ni or Sn concentration while the Mn content is above 37% in Ni-Mn-Sn alloys.

Keywords: exchange bias, anisotropy, antiferromagnetism, ferromagnetism, blocking bias temperature, coercive field, exchange bias field

1. Introduction

From the discovery of exchange bias (EB) in CoO particle [1], more work has been done on this area both experimentally and theoretically due to its potential applications in various fields such as spintronic devices, permanent magnets, magnetic recording, read head and giant magnetoresistive sensors, etc. [2–5]. EB arises in the presence of applied magnetic field after cooling the materials and it is connected with the exchange anisotropy formed at the interface between an antiferromagnetic (AFM) and ferromagnetic (FM) materials. The whole phenomenon at low temperature shifts the hysteresis loops along the field axis. This similar kind of phenomenon is observed in multilayer films, small oxide particles, nanostructures and inhomogeneous materials [6–9]. In addition to this, the EB phenomenon is also observed in materials which contains spin glass phase [10]. Recently, Ni-Mn-X (X = Ga, Sb, In, Sn) Heusler-based alloy systems achieved great attention due to their immense applications in magnetic refrigeration, magnetic actuated devices and spintronic devices [11, 12]. The different composition of Ni-Mn-Sn alloy shows a wide physical properties such as magnetic field-induced transition, inverse magnetocaloric effect (IMCE), giant magnetoresistance, giant Hall effect, giant magnetothermal conductivity, magnetic superelasticity effects, exchange bias and shape memory effect [13–17].

The recent observation of EB in the Ni-Mn-based alloys shows an intense interest in the further study of magnetic properties. Due to the different occupations of Mn atoms in the Sn sites as well in the Ni sites, the Ni-Mn-Sn alloy will have excess content of Mn atom. Hence the EB property is very sensitive to the excess Mn. The Ni_2MnSn Heusler alloy crystallizes in $L2_1$ structure, in which the Ni atoms occupy in

the (1/2, 1/2, 1/2) and (0, 0, 0) sites, Mn atoms occupy in the (1/4, 1/4, 1/4) site and Sn atoms occupy in the (3/4, 3/4, 3/4) site [18]. In the Mn-rich alloys, the excess Mn occupying Ni and Sn sites couples antiferromagnetically to surrounding Mn atoms on the regular Mn sites [19]. Also the decrease of Mn-Mn distance may lead to AFM exchange between each other in the martensite phase at low temperature. The EB behaviour has been studied in Ni-Mn-X (X = Sb, Sn, In) alloys by several authors [20–23]; particularly in Ni-Mn-Sn alloy, the EB behaviour has been investigated either by varying the Ni/Sn or Mn/Sn concentration [24, 25]. The structural effects, magnetic property and magnetic entropy change have been studied by varying Ni-Mn concentration in the $Ni_{50-x}Mn_{37+x}Sn_{13}$ ($0 \leq x \leq 4$) Heusler alloy system [26]. In the $Ni_{50-x}Mn_{37+x}Sn_{13}$ alloy system, the cubic austenite phase was stabilized by the excess Mn content at room temperature. The martensitic transition temperature decreases from 305 to 100 K by increasing the Mn concentration. The exchange bias blocking temperature (T_{EB}) was found to decrease drastically from 149 to 9 K with increasing Mn concentration. In this work, we have taken up a detailed study on the effect of varying Ni-Mn concentration on EB properties in the bulk $Ni_{50-x}Mn_{37+x}Sn_{13}$ alloys. This chapter explains the EB behaviour by varying Ni-Mn concentration in Ni-Mn-Sn alloys.

2. Experimental details

The compositions of $Ni_{50-x}Mn_{37+x}Sn_{13}$ (x = 0, 1, 2, 3, 4) alloys were prepared by arc melting technique under argon atmosphere. To ensure the homogeneity, the samples are re-melted four times. These alloys were annealed under high vacuum at 1175 K for 6 h and then quenched with Ar gas. The magnetic data were taken suing the physical property measurement system (PPMS-9 T)—vibrating sample magnetometer (VSM) module (Quantum Design, USA). The measurements were taken into two different modes which can be referred as ZFC and FC modes. The sample was firstly cooled in zero magnetic field, and the data was collected by applying a magnetic field of 5 mT during warming in the temperature range of 4–330 K. This refers to zero-field cooled (ZFC) mode. In field cooled (FC) mode, the data was collected without removing the applied field during cooling in the temperature range between 330 and 4 K. Again, the data was recorded upon warming in the range of 4–330 K (referred as field warming (FW)). Magnetization as a function of magnetic field was recorded up to a field of 5 T in the low temperatures.

3. Exchange bias behaviour of $Ni_{50-x}Mn_{37+x}Sn_{13}$ (x = 0, 1, 2, 3, 4) alloys

Figure 1 shows the temperature dependence of magnetization for $Ni_{50-x}Mn_{37+x}Sn_{13}$ (x = 0,1,2,3,4) alloys in an applied magnetic field of 5 mT during zero-field cooling, field cooling and field warming conditions. The curve shows several transitions with thermal hysteresis which has been observed between FC and FW. This thermal hysteresis is the indication of first-order structural transition from austenite to martensite phase. The ferromagnetic transition of austenite phase (T_C^A) occurs at 309 K. The decrease of magnetization below martensite start temperature (M_s) in the FC curve indicates the fractional decrease of austenite phase. The ZFC and FC curves split into two at low temperatures and show a step kind of behaviour in ZFC curve. This specifies that the sample is inhomogeneous magnetically. The transition observed at 120 K is referred as the exchange bias blocking temperature (T_{EB}). The observed magnetic inhomogeneity and T_{EB} in the sample can be attributed to the coexistence of FM and AFM interactions. This kind of antiferromagnetic interaction

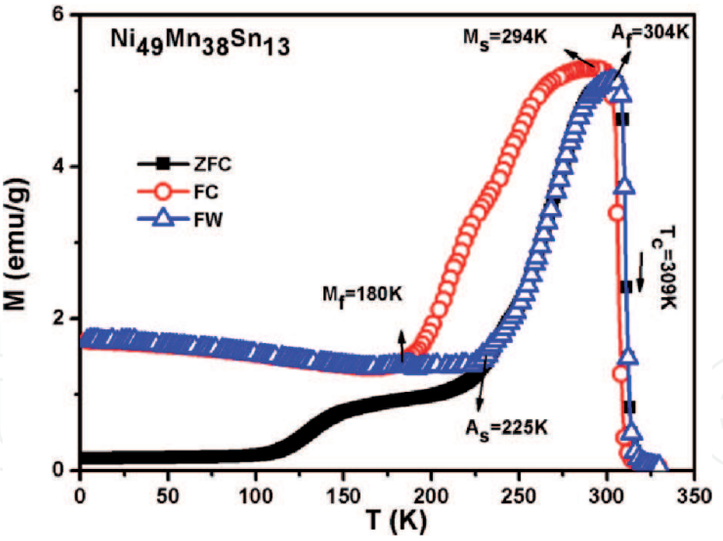

Figure 1.
ZFC, FC and FW thermomagnetic curves for $Ni_{49}Mn_{38}Sn_{13}$ alloy at a field of 5 mT.

occurs from the antiferromagnetic coupling between the Mn atoms in the Ni/Sn sites and Mn atoms in the Mn sites. The similar exchange bias behaviour is observed in further Ni-Mn-X (X = Sb, Sn, In) alloys [20–23]. The presence of AFM interaction in this alloy system was verified by neutron diffraction studies [27].

The ZFC and FC hysteresis loops were measured at 5 K to confirm the exchange bias in $Ni_{50-x}Mn_{37+x}Sn_{13}$ (x = 0, 1, 2, 3, 4) alloys. The ZFC and FC loops were measured from −20 kOe to 20 kOe. To measure the FC loop, the sample was cooled in a field of 50 kOe and recorded the loop from −20 kOe to 20 kOe. **Figure 2** shows the ZFC and FC hysteresis loops for $Ni_{50-x}Mn_{37+x}Sn_{13}$ (x = 0, 1, 2, 3, 4) alloys. The curves from −2 kOe to 2 kOe are shown in the inset in **Figure 3** to see the shift clearly. For all the samples, it is found that the ZFC curve does not exhibit any shift, but the FC curve shifts to the negative field from the origin. This specifies the coexistence of AFM-FM interactions in the sample below room temperatures. The ZFC loop shows a double-shifted loop and is symmetric around zero point, which indicates the existence of FM-AFM coupling. The emergence of double-shifted loop indicates that the different regions of AFM magnetic structure couple to the FM in opposite directions. The Ni-Mn-X (X = Sb, Sn, In) alloys also show similar EB behaviour [20–23].

The temperature dependence of EB was investigated in the temperature range of 5–140 K for $Ni_{50-x}Mn_{37+x}Sn_{13}$ (x = 0, 1, 2, 3, 4) alloys. The temperature interval has been taken as 20 K and the typical FC curves for $Ni_{50-x}Mn_{37+x}Sn_{13}$ (x = 1) alloy are shown in **Figure 3**. It is clear from **Figure 3** that at temperatures of 5 K and 20 K, the hysteresis loops significantly shifted to the negative field which point to the existence of EB in the sample. With the increase of temperature, the hysteresis loop decreases, and finally at 120 K the field shift almost disappears. The temperature where the loop is symmetric can be defined as the T_{EB} for this sample. Moreover, the temperature 120 K nearly coincides with the T_{EB} observed from the thermomagnetic data as shown in **Figure 2**.

Figure 4 shows the values of EB field (H_E) and coercivity (H_C) evaluated from the hysteresis loops at various temperatures for a typical $Ni_{50-x}Mn_{37+x}Sn_{13}$ (x = 1) alloy. The values of EB field and coercivity field are calculated using $H_E = -(H_1 + H_2)/2$ and $H_C = |H_1 - H_2|/2$, respectively, where H_1 and H_2 denote the negative and positive field at which the magnetization equals zero. It is observed from **Figure 4** that with increasing temperature the value of H_E decreases linearly and vanishes around T_{EB}. This validates the EB phenomenon to be real in the

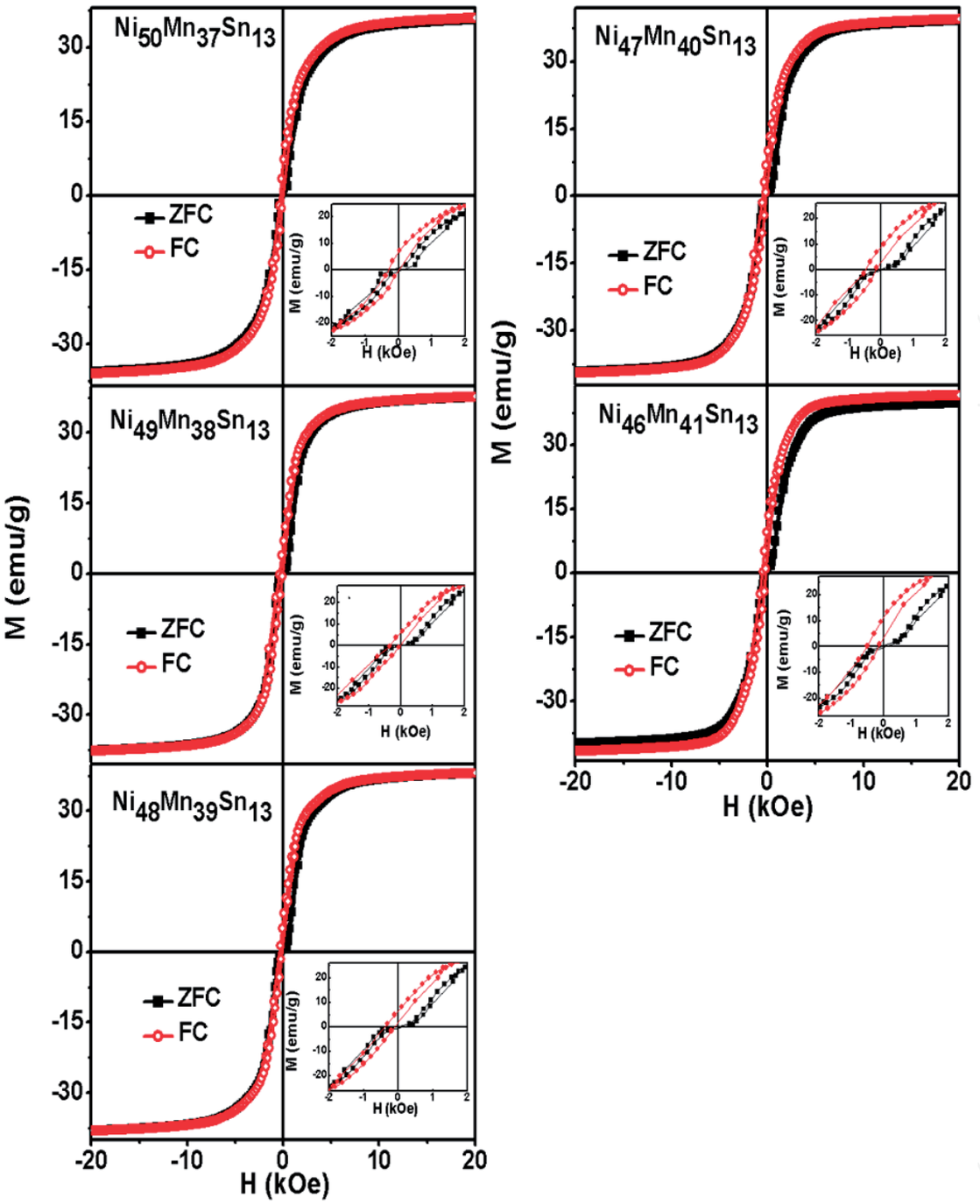

Figure 2.
Magnetic hysteresis loops obtained in the ZFC and FC mode for $Ni_{50-x}Mn_{37+x}Sn_{13}$ (x = 0, 1, 2, 3, 4) alloys at 5 K. inset shows the magnified image in low field range for better visibility of loop shift.

temperatures below T_{EB}. This is because with the increasing temperature, the FM-AFM coupling gets weakened. The disappearance of H_E is due to the domination of FM interaction over the AFM interactions. Conversely, H_C value increases in the beginning with temperature and decreases after reaching a maximum value. Due to the pulling of AFM spins by FM, the coercivity below T_{EB} increases. This arises due to the fact that anisotropy of AFM decreases with increasing temperature.

The T_{EB} values derived from the thermomagnetic curves (not shown for all samples) are plotted with Mn concentration for the alloys in **Figure 5**. From the figure it is seen that with the increase of Mn concentration from 37 to 41% in the $Ni_{50-x}Mn_{37+x}Sn_{13}$ alloy series, the T_{EB} decreases drastically from 149 to 9 K. The large fraction of FM phase at low temperature and the weakening of the

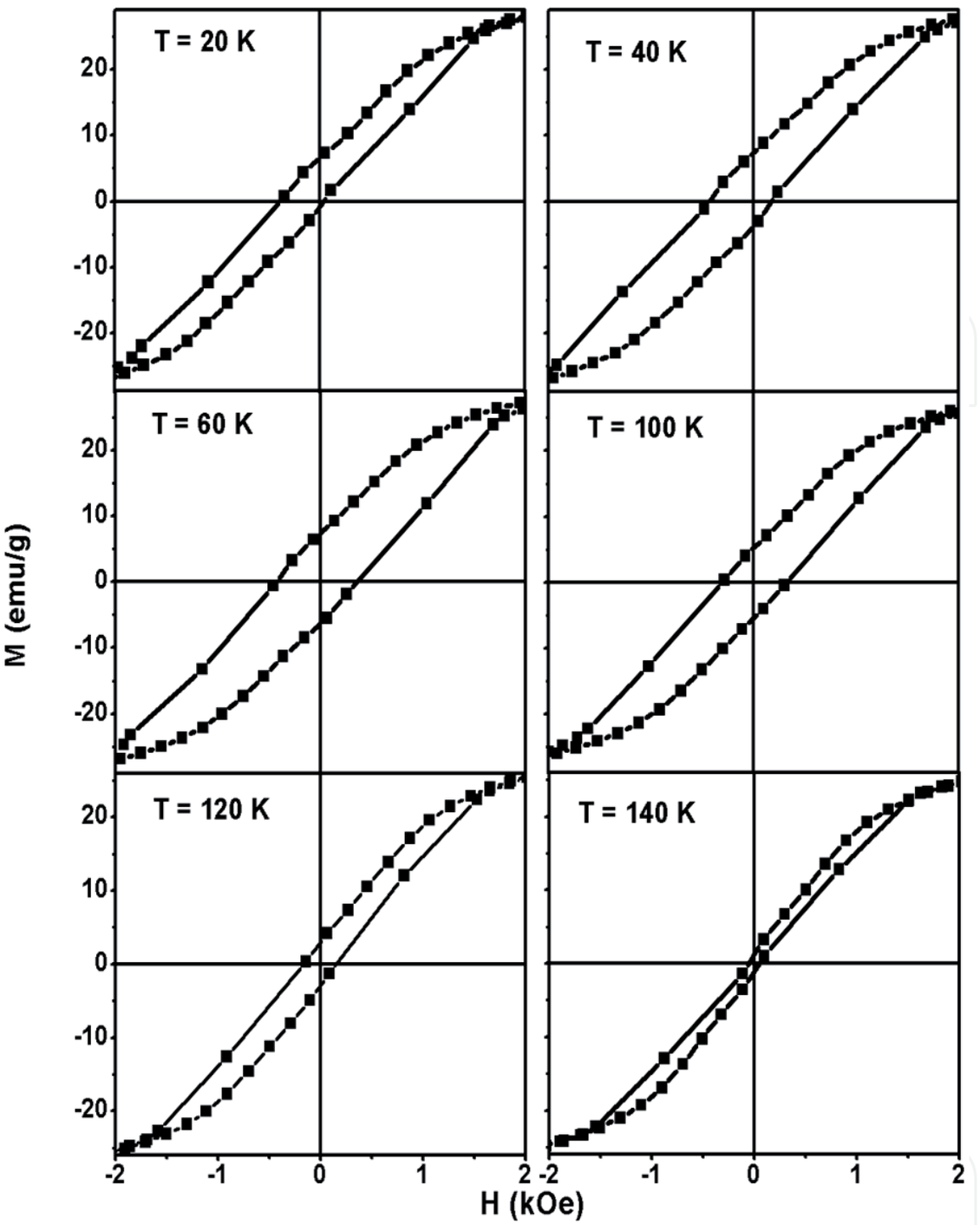

Figure 3.
FC magnetic hysteresis loops measured at various temperatures for $Ni_{49}Mn_{38}Sn_{13}$ alloy. Loop shift decreases with an increase of temperature.

AFM-FM interaction strength were verified by the experimental results which is shown in **Figure 5**, where the increase of Mn concentration increases the saturation magnetization (σ_s) at 5 K marginally. This indicates that the reduction in the FM-AFM interactions occurs due to the increase in Mn content. It can be understood that the weakening of the AFM interactions and the competing AFM and FM interactions led to the decrease of T_{EB} values. Earlier, M. Khan et al. reported the EB properties with varying Mn/Sn concentration in $Ni_{50}Mn_{50-x}Sn_x$ ($11 \leq x \leq 17$) alloys. In his work he reported that the increase of Mn concentration above 37% decreases the T_{EB} value [25]. Same in $Ni_{50-x}Mn_{37+x}Sn_{13}$ alloy series, the T_{EB} value was found to decrease with the increase of Mn content since the Mn

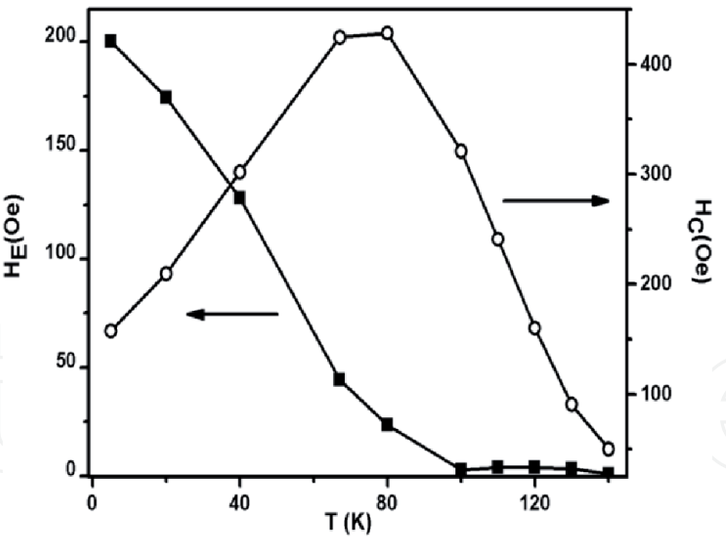

Figure 4.
Variation of EB field (H_E) and coercivity (H_C) with temperature for $Ni_{50-x}Mn_{37+x}Sn_{13}$ (x = 1) alloy.

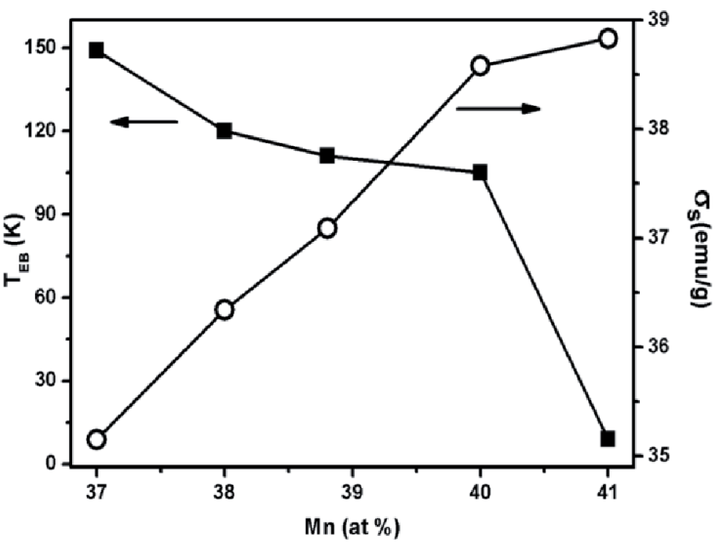

Figure 5.
Variation of T_{EB} and σ_s with Mn concentration in $Ni_{50-x}Mn_{37+x}Sn_{13}$ (x = 0, 1, 2, 3, 4) alloys.

content is more than 37% in $Ni_{50-x}Mn_{37+x}Sn_{13}$ alloy series. These results indicate that the T_{EB} value would decrease either by varying the Sn or Ni content if the Mn content is above 37% in Ni-Mn-Sn alloys.

The variation of H_E with the increase of Mn concentration is shown in **Figure 6** for $Ni_{50-x}Mn_{37+x}Sn_{13}$ alloy series at 5 K (calculated from **Figure 3**). It is noticed that with the increases of Mn concentration from 37 to 41%, the value of H_E increases linearly from 200 to 377 Oe. M. Khan et al. also observed the similar behaviour in Ni-Mn-Sn alloys and found that the H_E increases from ~20 to ~183 Oe with an increase of Mn from 34 to 39% by varying the Mn/Sn concentration [25]. These two results suggest that Ni-Mn variation greatly influences the H_E value in contrast to Mn/Sn variation. Recently, Xuan et al. reported EB by varying Ni/Sn concentration in Ni-Mn-Sn [keeping Mn concentration constant (50%)]. He observed that the increase of Sn content decreases the H_E field [24]. It indicates that the Mn occupying Sn and Ni sites plays a major role in modifying the magnetic interactions and their strength. It is reported that H_E depends on the interface coupling constant and saturation magnetization of the FM [28]. In the present $Ni_{50-x}Mn_{37+x}Sn_{13}$ alloy series, the different magnetic moments and interaction strength arises due to the

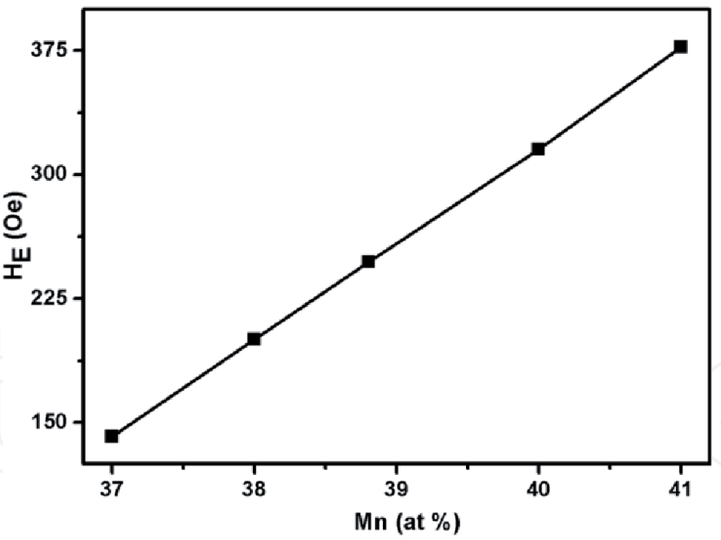

Figure 6.
Variation of EB field (H_E) with Mn concentration for $Ni_{50-x}Mn_{37+x}Sn_{13}$ (x = 0, 1, 2, 3, 4) alloys.

occupation of excess Mn in the Ni sites and Mn atoms occupies Sn and Ni. Hence the increase of H_E with increasing Mn could be due to the increase of interaction coupling strength of different moments in $Ni_{50-x}Mn_{37+x}Sn_{13}$ alloys. In order to understand the magnetic moment of different sites and their magnetic interactions in the sample, detailed neutron diffraction studies are essential.

4. Conclusion

In this chapter, we have discussed the exchange bias behaviour in $Ni_{50-x}Mn_{37+x}Sn_{13}$ (x = 0, 1, 2, 3, 4) alloys by changing the Ni-Mn concentration. The coexistence of AFM and FM exchange interactions is the reason for the EB phenomenon observed in this alloy series. The temperature strongly influences the H_E and H_C. The T_{EB} was found to be same for the Mn content more than 37%, even either varying Ni-Mn or Mn/Sn. With the increase of Mn concentration from 37 to 41%, the value of H_E increases linearly from 200 to 377 Oe in $Ni_{50-x}Mn_{37+x}Sn_{13}$ alloy series.

Acknowledgements

The authors would like to thank Dr. M. Manivelraja and Dr. N.V. Ramarao, DMRL, Hyderabad, India, for providing the facility for material synthesis.

Author details

Esakki Muthu Sankaran[1*] and Arumugam Sonachalam[2]

1 Department of Physics, Faculty of Arts Science and Humanities, Karpagam Academy of Higher Education, Coimbatore, India

2 Centre for High Pressure Research, School of Physics, Bharathidasan University, Tiruchirapalli, India

*Address all correspondence to: esakkimuthu.s@kahedu.edu.in

IntechOpen

References

[1] Meiklejohn WH, Bean CP. New magnetic anisotropy. Physics Review. 1956;**102**:1413-1414. DOI: 10.1103/PhysRev.102.1413

[2] Nogués J, Sort J, Langlais V, Skumryev V, Suriñach S, Muñoz JS, et al. Exchange bias in nanostructures. Physics Reports. 2005;**422**:65-117. DOI: 10.1016/j.physrep.2005.08.004

[3] Nowak U, Usadel KD, Keller J, Miltényi P, Beschoten B, Güntherodt G. Domain state model for exchange bias. I. Theory. Physical Review B. 2002;**66**:014430. DOI: 10.1103/PhysRevB.66.014430

[4] Nogués J, Schuller IK. Exchange bias. Journal of Magnetism and Magnetic Materials. 1999;**192**:203-232. DOI: 10.1016/S0304-8853(98)00266-2

[5] Kools JCS. Exchange-biased spin-valves for magnetic storage. IEEE Transactions on Magnetics. 1996;**32**:3165-3184. DOI: 10.1109/20.508381

[6] Stamps RL. Mechanism for exchange bias. Journal of Physics D. 2000;**33**:R247-R268. DOI: 10.1088/0022-3727/33/23/201

[7] Qian T, Li G, Zhang T, Zhou TF, Xiang XQ, Kang XW, et al. Exchange bias tuned by cooling field in phase separated $Y_{0.2}Ca_{0.8}MnO_3$. Applied Physics Letters. 2007;**90**:012503-1-3. DOI: 10.1063/1.2426887

[8] Fraune M, Rüdiger U, Güntherodt G, Cardoso S, Freitas P. Size dependence of the exchange bias field in NiO/Ni nanostructures. Applied Physics Letters. 2000;**77**:3815-3817. DOI: 10.1063/1.1330752

[9] Gruyters M. Spin-glass-like behavior in CoO nanoparticles and the origin of exchange bias in layered CoO/ferromagnet structures. Physical Review Letters. 2005;**95**:077204-1-4. DOI: 10.1103/PhysRevLett.95.077204

[10] Kodama RH, Makhlouf SA, Berkowitz AE. Finite size effects in antiferromagnetic NiO nanoparticles. Physical Review Letters. 1997;**79**:1393-1396. DOI: 10.1103/PhysRevLett.79.1393

[11] Planes A, Manosa L, Acet M. Magnetocaloric effect and its relation to shape-memory properties in ferromagnetic Heusler alloys. Journal of Physics. Condensed Matter. 2009;**21**:233201. DOI: 10.1088/0953-8984/21/23/233201

[12] Cong DY, Roth S, Pötschke M, Hürrich C, Schultz L. Phase diagram and composition optimization for magnetic shape memory effect in Ni–Co–Mn–Sn alloys. Applied Physics Letters. 2010;**97**:021908. DOI: 10.1063/1.3454239

[13] Rama Rao NV, Gopalan R, Chandrasekaran V, Suresh KG. Large low-field inverse magnetocaloric effect near room temperature in $Ni_{50-x}Mn_{37+x}In_{13}$ Heusler alloys. Applied Physics A: Materials Science and Processing. 2010;**99**:265-270. DOI: 10.1007/s00339-009-5517-3

[14] Yu SY, Liu ZH, Liu GD, Chen JL, Cao ZX, Wu GH, et al. Large magnetoresistance in single crystalline $Ni_{50}Mn_{50-x}In_x$ (x=14-16) upon martensitic transformation. Applied Physics Letters. 2006;**89**:162503. DOI: 10.1063/1.2362581

[15] Oikawa K, Ito W, Imano Y, Sutou Y, Kainuma R, Ishida K, et al. Effect of magnetic field on martensitic transition of $Ni_{46}Mn_{41}In_{13}$ Heusler alloy. Applied Physics Letters. 2006;**88**:122507. DOI: 10.1063/1.2187414

[16] Sozinov A, Likhachev AA, Lanska N, Ullakko K. Giant

magnetic-field-induced strain in NiMnGa seven-layered martensitic phase. Applied Physics Letters. 2002;**80**:1746-1748. DOI: 10.1063/1.1458075

[17] Hu FX, Shen BG, Sun JR. Magnetic entropy change in $Ni_{51.5}Mn_{22.7}Ga_{25.8}$ alloy. Applied Physics Letters. 2000;**76**:3460-3462. DOI: 10.1063/1.126677

[18] Kainuma R, Imano Y, Ito W, Sutou Y, Morito H, Okamoto S, et al. Magnetic-field-induced shape recovery by reverse phase transformation. Nature (London). 2006;**439**:957-960. DOI: 10.1038/nature04493

[19] Stager CV, Campbell CCM. Antiferromagnetic order in the Heusler alloy, $Ni_2Mn(Mn_xSn_{1-x})$. Canadian Journal of Physics. 1978;**56**:674-677. DOI: 10.1139/p78-085

[20] Khan M, Dubenko I, Stadler S, Ali N. Exchange bias behavior in Ni–Mn–Sb Heusler alloys. Applied Physics Letters. 2007;**91**:072510-1-3. DOI: 10.1063/1.2772233

[21] Li Z, Jing C, Chen JP, Yuan SJ, Cao SX, Zhang JC. Observation of exchange bias in the martensitic state of $Ni_{50}Mn_{36}Sn_{14}$ Heusler alloy. Applied Physics Letters. 2007;**91**:112505-1-3

[22] Jing C, Chen JP, Li Z, Qiao YF, Kang BJ, Cao SX, et al. Exchange bias behavior and inverse magnetocaloric effect in $Ni_{50}Mn_{35}In_{15}$ Heusler alloy. Journal of Alloys and Compounds. 2009;**475**:1-4. DOI: 10.1016/j.jallcom.2008.07.012

[23] Wang BM, Liu Y, Wang L, Huang SL, Zhao Y, Zhang H. Exchange bias and its training effect in the martensitic state of bulk polycrystalline $Ni_{49.5}Mn_{34.5}In_{16}$. Journal of Applied Physics. 2008;**104**:043916-1-4. DOI: 10.1063/1.2973187

[24] Xuan HC, Cao QQ, Zhang CL, Ma SC, Chen SY, Wang DH, et al. Large exchange bias field in the Ni–Mn–Sn Heusler alloys with high content of Mn. Applied Physics Letters. 2010;**96**:202502-1-3. DOI: 10.1063/1.3428782

[25] Khan M, Dubenko I, Stadler S, Ali N. Exchange bias in bulk Mn rich Ni–Mn–Sn Heusler alloys. Journal of Applied Physics. 2007;**102**:113914-1-4. DOI: 10.1063/1.2818016

[26] Esakki Muthu S, Rama Rao NV, Manivel Raja M, Raj Kumar DM, Mohan Radheep D, Arumugam S. Influence of Ni/Mn concentration on the structural, magnetic and magnetocaloric properties in $Ni_{50-x}Mn_{37+x}Sn_{13}$ Heusler alloys. Journal of Physics D: Applied Physics. 2010;**43**:425002-1-6. DOI: 10.1088/0022-3727/43/42/425002

[27] Aksoy S, Acet M, Deen PP, Manosa L, Planes A. Magnetic correlations in martensitic Ni-Mn-based Heusler shape-memory alloys: Neutron polarization analysis. Physical Review B. 2009;**79**:212401-1-4. DOI: 10.1103/PhysRevB.79.212401

[28] Meiklejohn WH. Exchange anisotropy—A review. Journal of Applied Physics. 1962;**33**:1328-1335. DOI: 10.1063/1.1728716